Influence of alloy disorder on the vibrational properties of Si/Ge superlattices

S. Wilke,* J. Mašek, and B. Velický
Institute of Physics, Czechoslovak Academy of Sciences, Na Slovance 2, CS-18040 Praha 8, Czechoslovakia
(Received 1 February 1989; revised manuscript received 21 September 1989)

A systematic study of the influence of disordered layers on the vibrational properties of Si/Ge superlattices is presented. The formalism used allows us to calculate the phonon Green function in the mixed representation for a superlattice with a general stacking of monolayers (presently along the ⟨001⟩ axis). The disordered layers are described within the coherent-potential approximation. Two arrangements of disordered layers in the superlattice are studied: thin interfacial alloy layers representing a diffuse interface and a superlattice whose one component is the Si-Ge alloy. Drastic suppression of superlattice quantum effects and the formation of modes induced by the alloy layers are predicted in both cases. The results show the sensitivity of the phonon spectrum of the superlattices to a long-range coherence of their chemical composition and to the perfection of their preparation.

I. INTRODUCTION

Superlattices (SL's) are one of the modern alternatives used in engineering device structures exhibiting low-dimensional phenomena. The quantum effects characterizing the SL systems arise from the change of material properties at the interfaces of an alternating sequence of heterojunctions. The behavior of the SL is determined not only by the chemical composition of the layers, but also by the layer thickness.

The dependence of the physical properties of the SL on the atomic arrangement is most clearly visualized in the spectrum of elementary excitations. Particularly pronounced effects are observed in the vibrational spectra of tetrahedral semiconductors. The reason for this is an isoelectronic substitution which is characteristic of the semiconductor SL. While the electronic structure is usually not changed very much, the phonon spectrum is strongly affected by the substitution since the involved atomic masses differ significantly in the isoelectronic case. An important feature of the spectra is the appearance of modes confined to only one component of the SL. These modes have been predicted theoretically and also observed by means of the Raman spectroscopy.[1–4]

The large difference of the atomic masses makes the phonon spectrum sensitive to the local bonding configurations and to fluctuations of the chemical composition. A typical example is the three-mode behavior of the phonon spectrum of Si-Ge alloys.[5] This raises an important question about the role of disordered (alloys) layers in the SL. The disordered layers are present not only in superlattices in which an alloy is intentionally used as one component of the SL, but always when the interfaces are not sufficiently abrupt. The alloys layers introduce their own spectral features. In addition, they destroy the long-range coherence of the waves. As long as the existence of the quantum SL effects requires the waves coherent over a region large compared with the SL period, an intense disorder scattering is expected to modify the behavior of the SL significantly. In the extreme case of an annealed SL, this may lead to a relaxation of all features specific to the SL, and the resulting SL spectrum then resembles a spectrum of the bulk alloy.

The influence of the alloy layers on both confined and propagative modes in the SL has been theoretically investigated only recently.[6,7] The quantitative calculations using the recursive method were performed for the case of the GaAs/(Ga,Al)As SL.[6] It was shown that the confinement of some modes can be largely reduced by the alloying. This unexpected feature was explained in connection with the fact that the spectrum of the (Ga,Al)As alloy has, in contrast to the spectrum of pure AlAs, an overlap with the optical-phonon branches in GaAs.

In this paper we present a systematic study of the phonon spectrum of the ⟨001⟩ Si/Ge SL with various arrangements of the disordered layers. The Si/Ge system has been selected not only for its practical importance, but also for its model character and simple short-range nature of the covalent bonding forces in this material. We develop a Green-function technique suitable for the calculation of various projections of the phonon density of states in superlattices with an arbitrary stacking sequence of monolayers. The Soven-Taylor coherent-potential approximation[8] (CPA) is generalized to the disordered layer structures and combined with an efficient recurrent procedure for calculating the matrix elements of the Green function. We also derive an expression for the averaged phonon spectral function. The theoretical formalism is described in Sec. II. The following results are discussed in Sec. III, which is divided into three subsections. In Sec. III A we start with the case of pure silicon and germanium crystals and with the Si/Ge SL consisting of perfect crystalline slabs. The main results, concerning two different arrangements of disordered layers in the Si/Ge SL, are presented in the other two subsections, and compared with the reference data obtained for the crystalline SL. In the first case, the disordered layers form a diffuse interface between the Si

and Ge slabs. The other arrangement corresponds to a Si/Si-Ge SL, where the Si-Ge alloy is used as one of the components of the SL.

II. THEORY

A. The model

We consider a general superlattice with alloy components and graded interfaces. It is defined by the chemical composition of a sequence of monolayers (labeled by i) along the SL axis, as specified by the concentration profiles $c_Q(i)$ of atomic species Q. In the periodic SL considered here the function $c_Q(i)$ is periodic with the SL period.

The local atomic arrangement in such a SL deviates in several respects from that found in the corresponding crystals. The most important change is a formation of an internal strain field due to the misfit of the lattice constant of the materials used as the SL components. The strain field may also be introduced by a partial ordering in the alloy layers. Other deviations from the ideal local atomic arrangement are caused by fluctuations of the chemical composition in the alloy. All these aspects of the atomic structure of a SL are reflected in the spectral properties of SL's, but we neglect them for the present and assume a perfect underlying lattice. This approximation is reasonable in the case of Si-Ge systems where the atomic masses of Si and Ge differ so much ($M_{\mathrm{Ge}}/M_{\mathrm{Si}}=2.6$) that both SL- and disorder-induced effects are caused mostly by the mass difference.

The phonon dispersion curves in the semiconductor crystals are, on a semiempirical level, described best within the bond-charge model.[9,10] It was shown that all essential interactions of the model are of a very short range for both Si and Ge; the remaining long-range part originating from the Coulomb ion-bond charge forces is unimportant.[10] The model can be fitted quantitatively well for simple crystals, but the transferability of its several parameters to more complex structures (alloys, amorphous semiconductors, and superlattices) is not trivial. Only the short-range nature of the forces can be assumed as long as the charge transfer between the atoms is negligible. This allows us to use a simpler Born model,[9,11] which has been widely used to describe the vibrational properties of disordered semiconductors.[5,12]

Under assumption only of the nearest-neighbor coupling, the deformation energy in the Born model consists of two terms:

$$V=\sum\frac{3\beta}{4}[(\mathbf{u}_I-\mathbf{u}_{I+\Delta})\cdot\mathbf{r}_\Delta(I)]^2+\sum\frac{\alpha-\beta}{4}(\mathbf{u}_I-\mathbf{u}_{I+\Delta})^2 . \tag{1}$$

These represent the central and noncentral (angular) forces acting in the covalent semiconductor lattice. The summation in Eq. (1) runs over all lattice sites I, $I+\Delta$ being one of four nearest neighbors of I. $\mathbf{u}_I$ is the displacement vector of an atom I and $\mathbf{r}_\Delta(I)$ is a unit vector directed along its Δth bond.

In parametrizing our model we made a further simplification by assuming the same force constants α,β for all Si—Si, Si—Ge, and Ge—Ge bonds. The similarity of the force constants in both crystals results from similar electronic structure and has been experimentally justified.[8] This restriction lowers the possibility of fitting the details of the dispersion relation in both Si and Ge, but it overcomes the problem of parametrizing the force constants in the alloy. The optimum values of the only two parameters, α and β, of the model fitted to the dispersion along the Γ–X direction in both pure crystals are $\alpha=51\ \mathrm{N\,m^{-1}}$ and $\beta=37\ \mathrm{N\,m^{-1}}$.

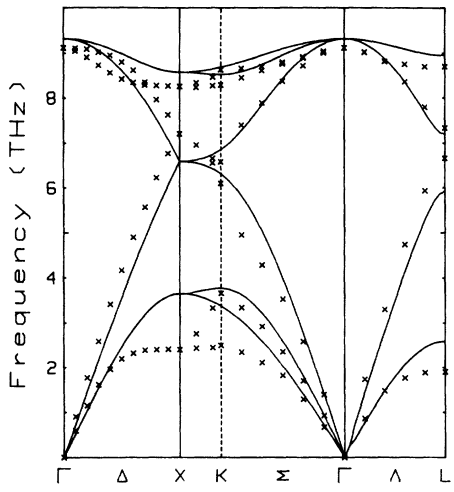

FIG. 1. Phonon dispersion relations for germanium as calculated within the Born model (solid lines). The crosses indicate experimental data from Ref. 13.

Figure 1 shows the phonon dispersion relations of germanium calculated for the Born model together with the experimental results.[13] It illustrates the basic features and limitations of the simply parametrized model we use. Although we assume the same force constants for both Ge and Si, the width of the photon spectrum of each of these two crystals is described reasonably well. The model is less satisfactory in those spectral regions where the noncentral forces are important, especially for the (TA) branch, as expected.[10] The fit can be partly improved by taking also the interactions between the next-nearest neighbors, but the profit from this becomes doubtful at the interfaces and particularly in the alloys.

B. Green functions

To calculate the phonon spectrum of the SL we use the Green-function formalism. The central quantities characterizing the spectrum are projected densities of states (PDOS's) which combine information about the energy distribution of modes and about their spatial behavior. The PDOS's are directly related to the diagonal elements of the Green-function matrix.

The dynamical behavior of the single-phonon processes is described by two different kinds of Green functions.[9] The displacement-displacement Green function G defined as

$$\underline{G}=(\underline{M}\omega^2-\underline{F})^{-1} \quad (2)$$

is related to the Raman and infrared-absorption spectra. The diagonal matrix $\underline{M}$ contains the masses of the atoms forming the SL, and $\underline{F}$ denotes the matrix of force constants [second derivatives of the deformation energy V, Eq. (1)]. ω is the angular frequency. The normalized density of the modes is determined by the displacement-momentum Green function $\underline{g}$,

$$\underline{g}=2\omega(\omega^2-\underline{1}-\underline{D})^{-1} . \quad (3)$$

where $\underline{D}=\underline{M}^{1/2}\underline{F}\,\underline{M}^{1/2}$ denotes the dynamical matrix of the system. The relation between these two Green functions is

$$\underline{g}=2\omega\underline{M}^{1/2}\underline{G}\,\underline{M}^{1/2} . \quad (4)$$

In the case of the SL containing disordered layers, the physically meaningful quantities are the Green functions averaged over all possible atomic configurations consistent with the concentration profile $c_Q(i)$. Assuming that the disorder is homogeneous in the layers perpendicular to the SL axis, the averaged Green function has the symmetry of the underlying SL structure. This is important because then the calculational procedure developed for an ideal SL without disorder can be used also in the case of disordered layers to obtain the averaged physical quantities.

To describe the spectral properties of the SL, we use a mixed representation which is natural for systems with two-dimensional periodicity. We introduce two-dimensional Bloch waves labeled by the wave vector $K=(k_x,k_y)$ and use the basis of Bloch waves also in the case of an alloy. The transformation to the Bloch representation is not done in the direction of the SL axis and the use of the layer index i is retained. Because of the periodicity in the layers (at least after the averaging) all quantities of interest are diagonal in K, and for each K we can decompose the spectrum into the contributions of individual layers i. Finally, we distinguish between the vibrations in different directions labeled by the Cartesian coordinate μ of the atomic displacement vector. This defined the projections we use.

The corresponding (K,i)-resolved densities of states (DOS's) $n_i(K,\omega)$ are related to the diagonal element of the displacement-momentum Green function g [see Eq. (3)]. In the general case we take the averaged Green function so that

$$n_i(K,\omega)=\frac{-1}{3\pi}\mathrm{Im}\sum_{\mu=1}^{3}\langle g_{i\mu\,i\mu}(K,\omega+i0)\rangle . \quad (5)$$

The factor $\frac{1}{3}$ guarantees the normalization of the DOS to unity and we use $\langle\cdots\rangle$ to denote the averaged quantities.

The local DOS at the site $I=(m,n,i)$ is related to the local projection of the Green function in the same way. The diagonal element of the Green function in the site representation corresponding to an atomic site (m,n) in the layer i can be constructed by the Fourier transformation. This reduces to the integration over the two-dimensional Brillouin zone (BZ) in the case of the diagonal elements,

$$g_{I\mu\,I\mu}(\omega)=\int_{\mathrm{BZ}}\frac{d^2K}{(2\pi)^2}g_{i\mu\,i\mu}(K,\omega) . \quad (6)$$

$g_{I\mu\,I\mu}(\omega)$ does not depend on the indices m,n. This reveals the two-dimensional homogeneity of the SL. An analogous relation also holds for the displacement-displacement Green function,

$$G_{I\mu\,I\mu}(\omega)=\int_{\mathrm{BZ}}\frac{d^2K}{(2\pi)^2}G_{i\mu\,i\mu}(K,\omega) . \quad (7)$$

C. The layer-dependent CPA

In the case of SL's with disordered layers we are interested in the configurationally averaged Green function. To obtain this quantity we use the CPA approach of Taylor[8] which can be applied to the alloys with pure mass disorder. We have only to generalize the CPA to a layer-dependent form appropriate for the inhomogeneous SL structure and to perform the averaging of the matrix elements of the Green-function diagonal in the mixed rather than in the commonly used site representation.

In applying the CPA to the phonons it is important to comment first on the different ways the mass disorder is represented in the two Green functions $\underline{G}$ and $\underline{g}$. The dynamical matrix $\underline{D}$ in the definition (3) of $\underline{g}$ exhibits a multiplicative two-center disorder. The problems connected with the multiplicative disorder, or equivalently with averaging the products of three random matrices in Eq. (4), have been solved recently[14] for the case of the electronic structure. We proceed in the same way and apply the CPA to the displacement-displacement Green function $\underline{G}$ which is expressed in terms of the diagonal mass matrix $\underline{M}$. Only at the end of the calculation do we transform $\langle\underline{G}\rangle$ into $\langle\underline{g}\rangle$ by using a modified Eq. (4).

The generalization of the CPA to the SL case is straightforward. The distribution of atoms in the SL, according to the arbitrary concentration profile $c_Q(i)$, is assumed homogeneous in each layer so that the averaged Green function $\langle\underline{G}\rangle$ is diagonal in K. $\langle\underline{G}\rangle$ corresponds to some effective SL with atomic masses replaced by frequency-dependent complex coherent mass functions $M^c_{i\mu\nu}(\omega)$ forming a block-diagonal coherent mass matrix $M^c(\omega)$. They have to be determined self-consistently. In contrast to the case of an isotropic bulk alloy, the coherent masses are not the same for all lattice sites but depend on the layer index i. This behavior reflects the microscopic one-dimensional inhomogeneity of the SL. It is important to note that even in the case of the constant-concentration profile within the alloy slabs of the $Si/Si_{1-x}Ge_x$ SL the coherent-mass function in the alloy layers depends on the distance from the interface and is not equal to the coherent-mass function of the bulk $Si_{1-x}Ge_x$ alloy. For those layers of the SL, where no mass disorder is present, the coherent mass reduces to the corresponding atomic mass.

Another feature connected with the anisotropy of the SL is that the atoms in the effective SL are not characterized by a single mass function. At least longitudinal and transverse masses must be distinguished. Generally, we

have to consider (3×3) blocks formed by $M^c_{i\mu\nu}(\omega)$. To simplify the notation we drop the Cartesian indices μ and join the matrix elements differing only in μ into blocks $M^c_i(\omega)$. In what follows we shall use this block representation also for all other quantities.

With this convention, the averaged Green function can be written as

$$\langle G_{ii}(K,\omega)\rangle=\{[\underline{M}^c(\omega)\omega^2-\underline{F}(K)]^{-1}\}_{ii} , \tag{8}$$

where $\underline{F}(K)$ is the appropriate projection of the force-constant matrix $\underline{F}$.

The CPA condition for the coherent mass $M^c_i(\omega)$ is formulated in terms of the site-diagonal matrix elements $\langle G_{II}(\omega)\rangle$ of the averaged Green function. For a site $I=(m,n,i)$ belonging to the layer i, this is obtained by applying the Fourier transform [Eq. (7)]. We point out again that $\langle G_{II}(\omega)\rangle$ does not depend on the actual position of the site I but only on the layer index i. Now we introduce an auxiliary function $\Omega_i(\omega)$. which describes the influence of the surroundings of the vibrations of the atom I (see Ref. 14), by writing the local Green functions in the form

$$\langle G_{II}(\omega)\rangle=[M^c_i(\omega)\omega^2-\Omega_i(\omega)]^{-1} . \tag{9}$$

This form of $\langle G_{II}(\omega)\rangle$ is particularly well suited for the formulation of the CPA self-consistency condition. Namely, if we fix an atom Q at site I, the corresponding conditionally averaged local Green function $\langle G^Q_{II}(\omega)\rangle$ is

$$\langle G^Q_{II}(\omega)\rangle=[M^Q\omega^2-\Omega_i(\omega)]^{-1} . \tag{10}$$

The CPA condition is that $\langle G_{II}(\omega)\rangle$ is just the averaged value of $\langle G^Q_{II}(\omega)\rangle$:

$$\langle G_{II}(\omega)\rangle=\sum_Q c_Q(i)\langle G^Q_{II}(\omega)\rangle . \tag{11}$$

Equations (8)–(11) together with (7) define the self-consistent coherent-mass functions. They have to be solved iteratively by calculating, in every step, the (K,i) projections of the averaged Green function of the effective SL and integrating them over the two-dimensional Brillouin zone according to (7). In contrast to the bulk alloy, the self-consistency must be carried out for all nonequivalent layers of the SL.

The local densities of states $n(I,\omega)$ are related to the diagonal elements of the average displacement-momentum Green function $\langle g(\omega)\rangle$, which can easily be constructed as a weighted average of the "impurity" Green functions $\langle G^Q_{II}(\omega)\rangle$ with the corresponding atomic masses M^Q:

$$n(I,\omega)=-\frac{2\omega}{3\pi}\mathrm{Im}\left[\sum_Q\sum_\mu c_Q(i)M^Q\langle G^Q_{I\mu I\mu}(\omega)\rangle\right] . \tag{12}$$

The problem of central importance is to obtain the spectral properties defined in (K,ω) space, reflecting the macroscopic symmetry of the SL. As long as we are not dealing with the site-diagonal elements, the averaged Green-function matrix $\langle \underline{g}\rangle$ cannot be constructed from $\langle \underline{G}\rangle$ in a simple way analogous to Eq. (12). The multiplicative form of the mass disorder in the dynamical matrix $\underline{D}$ which appears in the definition of g, however, makes it possible to find an explicit relation between $\langle \underline{g}\rangle$ and $\langle \underline{G}\rangle$ within the CPA. This relation has recently been derived for the electronic Hamiltonian.[4] The close analogy between the tight-binding Hamiltonian and the Born model used in the present work allows us to write a matrix equation for the Green function $\langle \underline{g}\rangle$,

$$\langle \underline{g}(\omega)\rangle=2\omega[\underline{\mathscr{C}}(\omega)\langle \underline{G}(\omega)\rangle\underline{\mathscr{C}}(\omega)+\underline{\mathscr{D}}(\omega)] . \tag{13}$$

A derivation of Eq. (13) is given in the Appendix. The matrices $\underline{\mathscr{C}}$ and $\underline{\mathscr{D}}$ are diagonal in the site representation and their matrix elements depend on the layer index i,

$$\mathscr{C}_i(\omega)=\frac{1}{M^A-M^B}\{[M^A-M^c_i(\omega)](M^B)^{1/2}+[M^B-M^c_i(\omega)](M^A)^{1/2}\} , \tag{14}$$

$$\mathscr{D}_i(\omega)=\left[\frac{(M^A)^{1/2}-(M^B)^{1/2}}{M^A-M^B}\right][c_A(i)M^A+c_B(i)M^B-M^c_i(\omega)]/\omega^2 . \tag{15}$$

The diagonal elements of the matrix $\langle \underline{g}\rangle$ in the mixed representation, which determine the (K,i)-resolved DOS, are obtained from (13) in the form

$$\langle g_{ii}(K,\omega)\rangle=2\omega[\mathscr{C}_i(\omega)\langle G_{ii}(K,\omega)\rangle\mathscr{C}_i(\omega)+\mathscr{D}_i(\omega)] , \tag{16}$$

where the two-dimensional Fourier transform was easily performed since the matrix elements of $\mathscr{C}$ and $\mathscr{D}$ are constant within each layer.

D. Evaluation of the Green function

In this subsection we describe the method used to calculate the matrix elements of the Green function in the mixed representation [cf. Eq. (8)]. We state again that the modes with different wave vectors K are completely decoupled from one another because of the periodicity of the (effective) SL. The three-dimensional problem reduces to a set of one-dimensional chains labeled by K. All chains representing a given SL have the same structure, schematically shown in Fig. 2(a), and are characterized by the same periodic sequence of atomic masses. The inversion appearing at the right-hand side of Eq. (8) can be straightforwardly done by using the large unit cell of the SL. Such an approach to the CPA in the superlattices was recently suggested by Ting and Chang.[15] Their formulation of the CPA involves the manipulation of large matrices and simplifying approximations must be used.

We do not follow this method but instead we combine the CPA with the recursive procedure which takes advantage of the local nature of the mass disorder, and of the finite range of the interactions between layers (nearest neighbors in our case). The local properties of a monolayer are then determined by two factors: the forces acting within the layer, and the influence of all other layers which can be treated by using various dialects of the "partitioning" technique. One possibility is to use the

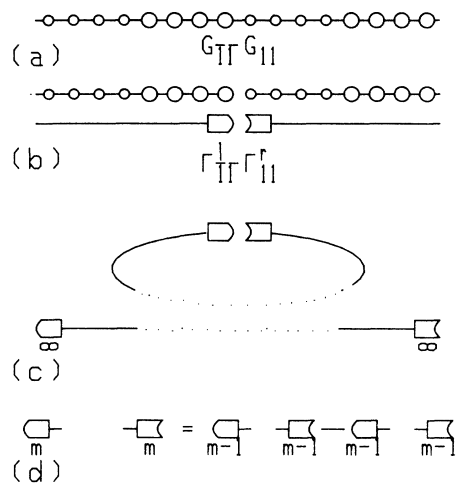

FIG. 2. Schematic representation of the calculational procedure (for details see text).

transfer-matrix method[16,17] or the renormalized projections of the Hamiltonian.[18] We do not use such a recurrence procedure in its simple form, but instead combine it with the layer-doubling scheme[19] which allows us to reduce the computational effort in the case of a SL with a long period.

To calculate the projections $G_{ii}(K,\omega)$ we proceed in two steps. First, the SL is cut at an interface and the projections of the Green function on the surface layers (terminal atoms of the chains) are calculated [see Fig. 2(b)]. The direction in which the semi-infinite chains are terminated are symbolically labeled by l and r. The corresponding surface Green functions are denoted by Γ^r_{11} and Γ^l_{11}. For simplicity, we drop the arguments K and ω where it does not lead to confusion. The surface Green functions are calculated by a recursive procedure (cf. Ref. 19), and used in the second step to construct all matrix elements $G_{ii}(K,\omega)$ layer by layer.

To calculate the surface Green function we apply arguments similar to the Born–von Kármán periodic boundary conditions and imagine that the SL is defined on a circle containing n periods [see Fig. 2(c)]. The cut SL is then represented by finite chains. As long as the chains are finite, both surfaces interact and we have to consider also the matrix elements of the Green function connecting both surface sites. Let us denote the projection of the Green function onto the space spanned by both surface sites of such a chain,

$$\underline{\Gamma}_{(n)}=\begin{bmatrix}\underline{\Gamma}^{rr}_{(n)} & \underline{\Gamma}^{rl}_{(n)}\\ \underline{\Gamma}^{lr}_{(n)} & \underline{\Gamma}^{ll}_{(n)}\end{bmatrix} . \tag{17}$$

With this notation, we have $\Gamma^r_{11}=\Gamma^{rr}_{(\infty)}$, $\Gamma^l_{11}=\Gamma^{ll}_{(\infty)}$, $\Gamma^{rl}_{(\infty)}=\Gamma^{lr}_{(\infty)}=0$. To perform the limit $n\to\infty$ we use a recursion cycle in which two chains are connected to form a longer chain, and the Green function $\Gamma_{(n)}$ is renormalized correspondingly. This is illustrated in Fig.2 (d).

Let us assume that we have constructed a chain containing one SL period. We now connect two of them to form a chain two periods long, then four, etc. The pth step represents a slab of 2^p periods and the Green functions converge rapidly. Also the first SL period, entering the iteration process above, can be constructed in the same way by sticking the chains which, in general, have different thicknesses and different atomic compositions.

The first step of the procedure consists of constructing a biatomic chain. The corresponding Green function is given by

$$\underline{\Gamma}_{(2)}=\left[\begin{bmatrix}\underline{M}^r\omega^2-\underline{F}^{rr} & \underline{0}\\ \underline{0} & \underline{M}^l\omega^2-\underline{F}^{ll}\end{bmatrix}-\begin{bmatrix}\underline{0} & \underline{F}^{rl}\\ \underline{F}^{lr} & \underline{0}\end{bmatrix}\right]^{-1} . \tag{18}$$

Here $\underline{F}^{ll}$ and $\underline{F}^{rr}$ are the projections of the force-constant matrix $\underline{F}(K)$ and the atomic sites at the surfaces l and r of the chain, and $\underline{F}^{rl}=(\underline{F}^{lr})^{\dagger}$ are the force constants between them.

In deriving the stacking formula describing the renormalization of the Green function when two chains with n and m layers are connected, we introduce the transition matrix related to the coupling between the two chains. The interaction V connects, say, the surface layer r of the chain containing m atoms with the surface l of the chain containing n atoms,

$$\underline{V}=\begin{bmatrix}\underline{0} & \underline{F}^{lr}\\ \underline{F}^{rl} & \underline{0}\end{bmatrix} . \tag{19}$$

The transition matrix $\underline{T}_{(m,n)}$ corresponding to the interaction $\underline{V}$ is, according to the standard scattering theory,

$$\underline{T}_{(m,n)}\equiv\begin{bmatrix}\underline{T}^{ll}_{(m,n)} & \underline{T}^{lr}_{(m,n)}\\ \underline{T}^{rl}_{(m,n)} & \underline{T}^{rr}_{(m,n)}\end{bmatrix}=\underline{V}(\underline{1}-\underline{\Gamma}_{(m,n)}\underline{V})^{-1} , \tag{20}$$

with

$$\underline{\Gamma}_{(m,n)}\equiv\begin{bmatrix}\underline{\Gamma}^{ll}_{(M)} & \underline{0}\\ \underline{0} & \underline{\Gamma}^{rr}_{(n)}\end{bmatrix} . \tag{21}$$

The renormalized surface Green functions are obtained by solving the corresponding Dyson equations

$$\begin{aligned}
\underline{\Gamma}^{rr}_{(m+n)}&=\underline{\Gamma}^{rr}_{(m)}+\underline{\Gamma}^{rl}_{(m)}\underline{T}^{ll}_{(m,n)}\underline{\Gamma}^{lr}_{(m)} ,\\
\underline{\Gamma}^{rl}_{(m+n)}&=\underline{\Gamma}^{rl}_{(m)}\underline{T}^{lr}_{(m,n)}\underline{\Gamma}^{rl}_{(n)} ,\\
\underline{\Gamma}^{lr}_{(m+n)}&=\underline{\Gamma}^{lr}_{(n)}\underline{T}^{rl}_{(m,n)}\underline{\Gamma}^{lr}_{(m)} ,\\
\underline{\Gamma}^{ll}_{(m+n)}&=\underline{\Gamma}^{ll}_{(n)}+\underline{\Gamma}^{lr}_{(n)}\underline{T}^{rr}_{(m,n)}\underline{\Gamma}^{rl}_{(n)} .
\end{aligned} \tag{22}$$

The second step is the calculation of the diagonal matrix elements of the Green function $G_{ii}(K,\omega)$ from the knowledge of surface Green functions Γ^r_{11} and Γ^l_{11}. This is demonstrated for layer 1 [see Fig. 2(a)]. The partitioning to the matrix element G_{11} (for each K) is given by

$$\underline{G}_{11}=(\underline{M}_1\omega^2-\underline{F}_{11}-\underline{F}_{12}\underline{\Gamma}^{l}_{22}\underline{F}_{21}-\underline{F}_{11}\underline{\Gamma}^{r}_{11}\underline{F}_{11})^{-1} . \tag{23}$$

Here $\underline{F}_{ij}$ denotes (3×3) submatrices of the force-

constant matrix $\underline{F}(K)$ between layers i and j. The application of Eq. (23) requires the knowledge of the surface Green function $\underline{\Gamma}^{l}_{22}$ belonging to the cut between layers 1 and 2. Using the partitioning again, we obtain an implicit relation for $\underline{\Gamma}^{l}_{22}$,

$$\underline{\Gamma}^{l}_{11}=(\underline{M}_{1}\omega^2-\underline{F}_{11}-\underline{F}_{22}\underline{\Gamma}^{l}_{22}\underline{F}_{21})^{-1}\ , \tag{24}$$

which can easily be inverted. Equations (22) and (23) are sufficient to calculate $\underline{G}_{11}$. To calculate $\underline{G}_{22}$ we also need the Green function:

$$\underline{\Gamma}^{r}_{11}=(\underline{M}_{1}\omega^2-\underline{F}_{11}-\underline{F}_{11}\underline{\Gamma}^{r}_{11}\underline{F}_{11})^{-1}\ . \tag{25}$$

Repeated application of the equations analogous to (22)–(25) is used to calculate the matrix elements of the Green function at all layers. The resulting (K,i)-resolved DOS is given by Eq. (5).

III. RESULTS

A. The ideal Si/Ge superlattices

We investigate a symmetric ⟨001⟩ SL with a SL period of 16 monolayers. The (K,i)-resolved DOS is calculated at the Γ point of the two-dimensional Brillouin zone. This point represents the projection of the dispersion relation along the SL axis and is therefore well suited to show the quantum effects arising from the SL periodicity. The transverse and longitudinal modes decouple at this point, and the linear-chain model can directly be applied to the crystalline SL as done in Refs. 7, 19, and 20.

We start with the (K,i)-resolved DOS for pure silicon and germanium crystals for $K=(0,0)$. This quantity is shown in Fig. 3. It can be obtained by integrating the spectral function along the Γ–X line in the three-dimensional Brillouin zone (see Fig. 1). The spectra of the two materials are related one to another by a simple scaling

$$n_i^{\mathrm{Si}}(K,\omega)=n_i^{\mathrm{Ge}}(K,(M_{\mathrm{Si}}/M_{\mathrm{Ge}})^{1/2}\omega)\ , \tag{26}$$

and have a form typical for the one-dimensional bands with sharp peaks at the band edges. The existence of two sublattices is reflected in a down-folding of a longitudinal band. The transverse modes form two separate bands: the TA branch corresponds to the bond-bending vibrations, the narrow (TO) band is formed by the stretching modes.

Both materials are now combined to form an (8,8) Si/Ge SL, $(Si_8)/(Ge_8)$. Figure 4 shows the corresponding (K,i)-resolved DOS at all nonequivalent layers for both transverse and longitudinal modes, respectively. In accordance with Ref. 19 we distinguish the spectral regions of extended and confined modes. The extended modes, belonging to the spectral range where the silicon and germanium bands overlap, are characterized by the formation of minibands separated by small gaps. The difference between the silicon and germanium spectra increases with increasing frequency and this is reflected in the decreasing dispersion of the minibands and in the widening of the gaps between them. Most of the region of the extended states can be described within a continuum approximation.[21]

The confined modes have a very short penetration depth into the barrier layers. They can be described by standing waves inside the slab and are determined essentially by the bulk properties of the corresponding material. The standing waves correspond to the wave vectors

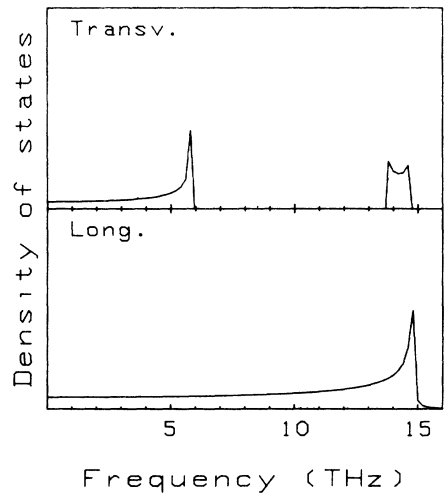

FIG. 3. (K,i)-resolved density of vibrational states of Si (dashed lines) and Ge (dotted lines) projected on the Γ point of the ⟨001⟩-layer Brillouin zone.

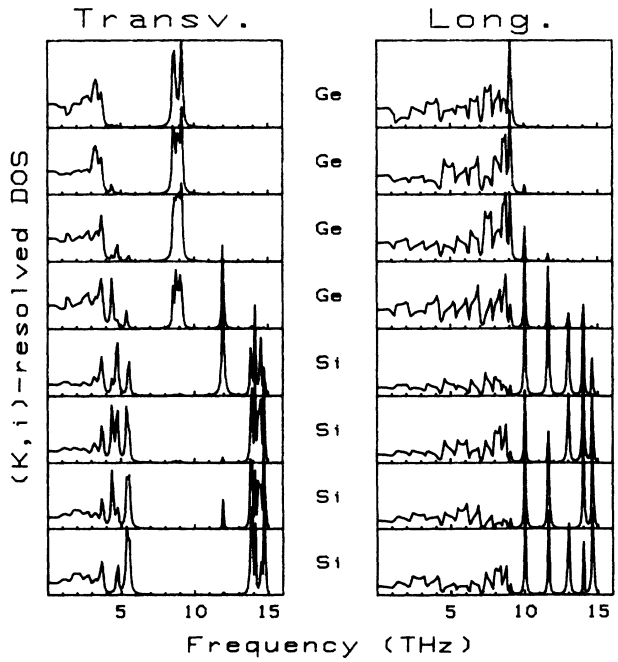

FIG. 4. (K,i)-resolved density of vibrational states of the (8,8) ⟨001⟩ Si/Ge crystalline superlattice at $K=(0,0)\pi/a$.

$$k_z = \frac{\pi}{nd} m, \quad m = 0, 1, \ldots, n/2 \tag{27}$$

where d is the monolayer spacing and n is the number of monolayers in the slab. The frequencies of these modes are given by unfolding the wave vectors into the bulk fcc Brillouin zone. This so-called "unfolded rule,"[20] predicting the existence of five separated confined modes, is illustrated well for the LO modes in Fig. 4.

An abrupt Si/Ge interface is characterized by the transverse interface mode at about 11.8 Thz.[4,19] It originates from the large change of the atomic masses at a monolayer distance, and represents vibrations localized mostly at the interfacial Si/Ge layers, with damped oscillations penetrating into the silicon slab.

B. The disordered interface layer

We consider now a Si/Ge SL with a diffuse interface. The SL is modeled by six Si and six Ge layers separated by two interfacial alloy layers of composition $Si_{0.7}Ge_{0.3}$ and $Si_{0.3}Ge_{0.7}$, respectively. The (K,i)-resolved DOS for such a SL is presented in Fig. 5. The results of the ideal counterpart (Fig. 4) are also shown for selected layers for comparison.

The effect of the disordered interfacial layers is different for different kinds of modes. The transverse modes are only slightly altered by the disorder scattering. This behavior can be explained by the fact that the transverse modes are determined largely by local symmetry within the slabs; due to their extreme confinement they do not respond sensitively to the changes at the interface. Apart from the disorder broadening, the frequency shift of the confined TA modes is well described by a barrier with a graded rather than steplike potential. A different situation is found near the interface. We observe that the interface mode survives, but its nature is modified. Formerly a vibration of the interface layer, it is now a collective vibration of number of layers in the interface region. Also its frequency is changed. The result confirms the conjecture that the true interface vibrations are characteristic of an abrupt interface.

Longitudinal modes confined in the silicon slab fill a wide spectral region and are strongly affected by the disorder at the interface. Figure 5 illustrates how much the scattering of the confined modes by the disordered interface relaxes the quantization which formerly lead to the standing waves. The envelope of the layer-resolved spectrum resembles the spectrum of the pure crystals in Fig. 3. Additional small peaks, indicating the position of quasiparticle standing-wave excitations, appear at frequencies corresponding to a Si (10) slab. It is known from the studies of the electronic structure that the graded interface with a linear dependence of the alloy composition exhibits confined states at nearly the same energies as the SL with an abrupt interface and with slabs thicker by about one-half of the interfacial region. We see that this conclusion is not valid now: the peaks characteristic for both Si (8) and Si (10) slabs are present, with reduced intensity, in Fig. 4.

Generally speaking, the effect of the disordered interfacial region can be understood as a reduced coherence of the waves. This becomes particularly produced for the optical modes and results in a relaxation of quantum effects induced by the SL. The two components of the SL then seem to be rather independent. The features related to the local symmetry within the slabs dominate over those induced by the SL, as demonstrated, e.g., by the absence of the first confined LO mode.

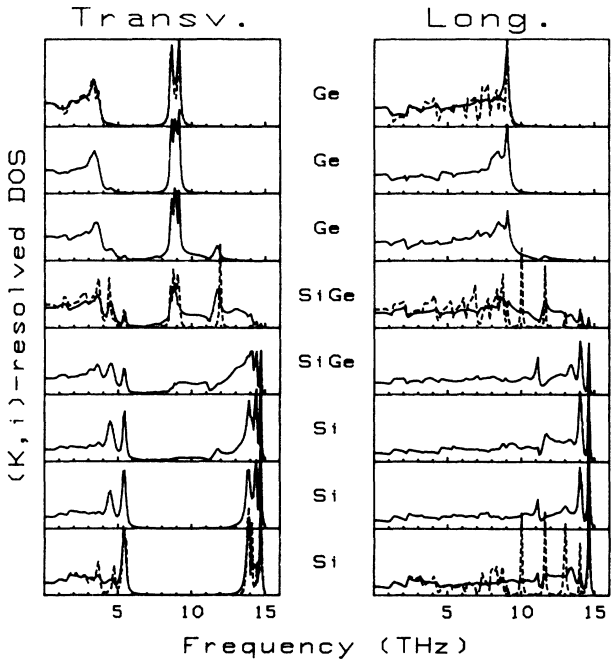

FIG. 5. The same as Fig. 4 for the (8,8) Si/Ge superlattice with graded interface (see text). The results from Fig. 4 are indicated at selected layers for comparison (dotted line).

C. The alloy superlattice

The other case that we consider is the Si/Si-Ge SL whose second component is the alloy. Such a SL has great practical importance, since the alloy composition is an additional free parameter controlling the properties of the SL. It is interesting to contrast the vibrational spectrum of the alloy SL to the results obtained in the preceding paragraphs. As a representative example we chose the $(Si)_8/(Si_{0.5}Ge_{0.5})_8$ SL assuming an abrupt interface between the silicon and alloy slabs. The continuous spectrum of (damped) excitations in the $Si_{0.5}Ge_{0.5}$ alloy extends over almost the whole silicon spectrum. The overlap between the $Si_{0.5}Ge_{0.5}$ spectrum and the bands of pure Si is therefore larger than for Ge and Si, and this makes the alloy layers "transparent" for the siliconlike excitations. The nature of the modes in this region depends on the localization of these modes in the alloy as well as on the thickness of the alloy slab.

Figure 6 shows the (K,i)-resolved spectrum of the superlattice. Again, the results for the reference Si/Ge SL are indicated by dashed lines. Comparing the behavior of

the transverse modes in silicon for both cases, we find a pronounced similarity in accordance with the arguments presented before. It is interesting to comment on the interfacial mode. It appears at the same frequency as for the Si/Ge SL, but does not show the characteristic peaks in the silicon slab. There are, however, small peaks in the alloy slab. We conclude from this that the interfacial mode has now a nature of an alloy mode, induced by the presence of adjacent pure-silicon layers. It is important to note that this mode will be, in reality, overlapped by a large density of local Si/Ge modes characteristic for the alloy,[5,22] but not accounted for in the present CPA calculations.

The behavior of the confined longitudinal modes depends on the frequency domains. In the middle of the range of the confined modes, approximately at 11.5–13 THz, the peaks corresponding to the standing waves in the Si/Ge SL are observed. In this region the quasiparticle excitations in the alloy are strongly damped. The alloy acts as a barrier, i.e., it has a similar role as Ge in the Si/Ge SL. The disorder scattering of the modes is reflected by the broadening of the peaks.

Near the germanium and silicon spectral bounds, on the other hand, the isolated peaks disappear and features resembling the minibands are found around the positions of the first and fourth confined LO modes. These modes reflect the "transparency" of the alloy layers to the siliconlike excitations predicted in Refs. 6 and 7.

At highest frequencies, namely above the edge of the continuous spectrum of the alloy, the true confined modes are formed. They have been observed in the Raman experiments.[4]

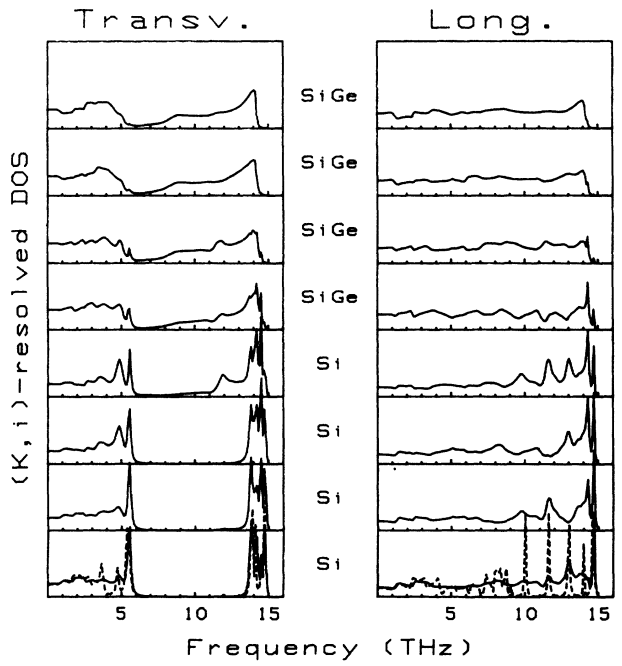

FIG. 6. The same as Fig. 4 for the (8,8) $Si/Si_{0.5}Ge_{0.5}$ superlattice. The results from Fig. 4 are indicated at selected layers for comparison (dotted line).

IV. CONCLUSIONS

We studied the influence of the disordered layers on the phonon spectrum in the silicon-based superlattices. The disorder in the alloy layers was described within the CPA generalized to the inhomogeneous SL structure and combined with an efficient scheme for calculating the diagonal elements of the Green function. In contrast to all previous CPA calculations, we were able to obtain not only the averaged local densities of states, but also the averaged spectral functions defined in the mixed (K,i) representation.

The calculations are based on the Born model as the simplest approximation for the lattice vibrations in homopolar covalent materials. The calculational method, however, does not depend on this choice and can easily be used also for more sophisticated short-range interaction models. The applicability of the method is also not restricted to the case of the simplified geometry of the SL which we used (neglected internal strains).

The application of our method to a crystalline Si/Ge SL with an abrupt interface reproduces well results obtained by other approaches.[19] In particular, we found standing wavelike excitations that are strongly confined because of the large difference between the atomic masses of Si and Ge. A local mode of Si—Ge vibrations was obtained at the abrupt interface.

Important novel features were obtained in the case of SL's containing disordered layers. The standing-wave excitations, typical for the SL arrangement, disappear in the presence of even a small number of disordered layers in the SL with diffuse interfaces. Individual slabs are then effectively decoupled one from another. This confirms the fact that the formation of quantum effects in SL requires abrupt interfaces and the coherence of the waves along the SL axis.

Two effects are found in the case when the alloy is used as one component of the SL. In regions of strong scattering and low penetration depth into the alloy, the alloy acts as a barrier for the siliconlike excitations. Near the bounds of the confined modes, on the other hand, the "transparency"[6,7] of the alloy to the siliconlike excitations is reflected in a series of localized modes, but with the DOS similar to a miniband.

When comparing the results with the Raman spectra,[4] it should be stressed that in this case the actual atomic positions and the incorporation of the strain field may be important. Therefore, we do not expect that the spectral densities presented here reproduce all details of the actual spectral distribution. This is partly connected with the limitation of the CPA as a single-site approximation. It described appropriately the damping of the Bloch waves in the alloy and the effects connected with the formation of the Si/Si-Ge SL, i.e., the features induced by alternation of the silicon and alloy layers. On the other hand, the CPA is not well suited to describe the local modes due to the specific bonding configuration even in the bulk alloy which exhibits a three-mode behavior.[5,22] To reproduce these features of the DOS in the alloy layers, cluster corrections have to be included. The structure of the DOS related to the modes at the local atomic configurations superimpose over the superlattice spec-

trum calculated within the CPA. This differential effect can be estimated quantitatively just by comparing the CPA calculations with the results of the cluster calculations.[5,12] The role of the internal strain could be estimated in the same way.

APPENDIX

It has already been stated in the text that the structure and the transformation [see Eq. (4)] between the phonon Green functions $\underline{g}$ and $\underline{G}$ is very similar to that of the Green function $\underline{g}$ and the auxiliary resolvent $\underline{G}$ studied in Ref. 14. In fact, only the analytical properties of the resolvents and the Dyson equation have been used to derive the relationship between both matrices averaged within the CPA. The steps taken in Ref. 14 can be repeated for the case of the phonon Green functions by making the following substitutions:

$$\begin{aligned} &W_0 \rightarrow \underline{D} \ , \\ &W \rightarrow \underline{F}_{IJ} \ , \\ &D \rightarrow \underline{F}_{II} \ , \\ &\alpha \rightarrow \underline{M}^{-1/2} \ , \\ &L(z) \rightarrow \underline{L}(\omega,i) = (\underline{M}\omega^2 - \underline{F}_{II}) \ , \\ &\mathcal{L}(z) \rightarrow \underline{\mathcal{L}}(\omega,i) = (\underline{M}^c\omega^2 - \underline{F}_{II}) \ , \\ &\Delta \rightarrow (M^A - M^B)\omega^2 \ . \end{aligned} \tag{A1}$$

In the case of the SL the locator $\underline{L}(\omega,i)$, as well as the masses of the alloy components, is dependent on the layer index i. The final expression of Ref. 14 can be rewritten for the phonon case by using projection operators $P_\mu(i)$ selecting the μth Cartesian coordinate of displacements in the layer i (all other symbols have the same meaning as in Ref. 14):

$$\begin{aligned} \langle g(\omega) \rangle = &\sum_{i,j} \sum_{\mu,\nu} \mathcal{C}_\mu(i) P_\mu(i) \langle G(\omega) \rangle P_\nu(j) \mathcal{C}_\nu(j) \\ &+ \mathcal{D}_\mu(i) P_\mu(i) \delta_{ij} \delta_{\mu\nu} \end{aligned} \tag{A2}$$

where we introduced diagonal matrices $\underline{\mathcal{C}}$ and $\underline{\mathcal{D}}$ with the matrix elements

$$\begin{aligned} \mathcal{C}_\mu(i) = \frac{1}{\Delta} (&(M^B)^{1/2} \{ [\underline{L}^A(i)]^{-1} - [\underline{\mathcal{L}}_\mu(i)]^{-1} \} \\ &- (M^A)^{1/2} \{ [\underline{L}^B(i)]^{-1} - [\underline{\mathcal{L}}_\mu(i)]^{-1} \}) \ . \end{aligned} \tag{A3}$$

$$\begin{aligned} \mathcal{D}_\mu(i) = \frac{[(M_A)^{1/2} - (M_B)^{1/2}]^2}{\Delta^2} \{ &c_A(i) [\underline{L}^A(i)]^{-1} \\ &+ c_B(i) [\underline{L}^B(i)]^{-1} \\ &- [\underline{\mathcal{L}}_\mu(i)]^{-1} \} \ . \end{aligned} \tag{A4}$$

The matrix notation introduced here replaces the summation used in Ref. 14. The explicit expression in Eqs. (13)–(15) is derived by using the relations (A1).

The site-diagonal elements of $\langle g \rangle$ appearing in Eq. (12) for the local DOS are obtained from (A2) by using the CPA equations in the form [we correct a misprint in Eq. (28) of Ref. 14]

$$\begin{aligned} \langle g_{II}(\omega) \rangle = \sum_Q c_Q(i) M^Q (\underline{1} + \{ &[\underline{L}^Q(i)]^{-1} - [\underline{\mathcal{L}}_\mu(i)]^{-1} \} \\ &\times \langle \underline{G}_{II}(\omega) \rangle)^{-1} \langle \underline{G}_{II}(\omega) \rangle \ . \end{aligned} \tag{A5}$$

The term in curly braces is rewritten by using Eqs. (9) and (10) and the final form presented in (12) is obtained.

*Permanent address: Department of Physics, Humboldt University, Berlin, Invalidenstrasse 110, DDR 1040 Berlin, DDR.

[1]A. S. Baker, J. C. Merz, and A. C. Gossard, Phys. Rev. B **17**, 3181 (1978).
[2]B. Jusserand, P. Paquet, and F. Alexandre, Surf. Sci. **174**, 94 (1986).
[3]D. Levi, S. L. Zhang, M. V. Klein, and H. Morkoç, Phys. Rev. B **36**, 8032 (1987).
[4]H. Brugger and G. Abstreiter, J. Phys. (Paris) Colloq. **48**, C5-321 (1987).
[5]F. Yndurain, Phys. Rev. Lett. **37**, 1062 (1976).
[6]A. Kobayashi and A. Roy, Phys. Rev. B **35**, 2237 (1987).
[7]B. Zhu and K. A. Chao, Phys. Rev. B **36**, 4906 (1987).
[8]D. W. Taylor, Phys. Rev. **156**, 1017 (1967); P. Soven, *ibid.* **156**, 809 (1967).
[9]H. Böttger, *Principles of the Theory of Lattice Dynamics* (Akademie Verlag, Berlin, 1983).
[10]W. Weber, Phys. Rev. B **15**, 4789 (1977).
[11]M. Born and K. Huang, *Dynamical Theory of Crystal Lattices* (Clarendon, Oxford, 1954).
[12]D. Beeman and R. Alben, Adv. Phys. **26**, 339 (1977).
[13]G. Nilsson and G. Nelin, Phys. Rev. B **3**, 364 (1971).
[14]J. Kudrnovský and J. Mašek, Phys. Rev. B **31**, 6424 (1985); J. Kudrnovský, V. Drchal, and J. Mašek, *ibid.* **35**, 2487 (1987).
[15]D. Z.-Y. Ting and Y.-C. Chang, Phys. Rev. B **37**, 8932 (1988).
[16]P. H. Lee and J. D. Joannopoulos, Phys. Rev. B **23**, 4988 (1981); **23**, 4997 (1981).
[17]J. N. Schulmann and Y.-C. Chang, Phys. Rev. B **27**, 2346 (1983); S. Yip and Y.-C. Chang, *ibid.* **30**, 7037 (1984).
[18]R. D. Graft, D. J. Lohrmann, G. P. Parravicini, and L. Resca, Phys. Rev. B **36**, 4782 (1987).
[19]A. Fasoloni and E. Molinari, J. Phys. (Paris) Colloq. **48**, C5-569 (1987).
[20]E. Molinari, A. Fasolino, and K. Kunc, Superlatt. Microstruct. **2**, 397 (1986).
[21]D. J. Lockwood, M. W. C. Dharma-wardana, J.-M. Baribeau, and D. C. Houghton, Phys. Rev. B **35**, 2243 (1987).
[22]J. S. Lannin, Phys. Rev. B **16**, 1510 (1977).
[23]M. I. Alonso and K. Winer, in *Proceedings of the Nineteenth International Conference on the Physics of Semiconductors, Warsaw, Poland, 1988,* edited by W. Zawadski (IOP, Polish Academy of Sciences, Warsaw, 1988), p. 815.